



12-3-2007

Hard Disks on the Hyperbolic Plane

Carl D. Modes
University of Pennsylvania

Randall D. Kamien
University of Pennsylvania, kamien@physics.upenn.edu

Follow this and additional works at: http://repository.upenn.edu/physics_papers

 Part of the [Physics Commons](#)

Recommended Citation

Modes, C. D., & Kamien, R. D. (2007). Hard Disks on the Hyperbolic Plane. Retrieved from http://repository.upenn.edu/physics_papers/119

Suggested Citation:

C.D. Modes and R.D. Kamien. (2007). "Hard Disks on the Hyperbolic Plane." *Physical Review Letters*. **99**, 235701.

© 2007 The American Physical Society
<http://dx.doi.org/10.1103/PhysRevLett.99.235701>

This paper is posted at Scholarly Commons. http://repository.upenn.edu/physics_papers/119
For more information, please contact repository@pobox.upenn.edu.

Hard Disks on the Hyperbolic Plane

Abstract

We examine a simple hard disk fluid with no long range interactions on the two-dimensional space of constant negative Gaussian curvature, the hyperbolic plane. This geometry provides a natural mechanism by which global crystalline order is frustrated, allowing us to construct a tractable model of disordered monodisperse hard disks. We extend free-area theory and the virial expansion to this regime, deriving the equation of state for the system, and compare its predictions with simulation near an isostatic packing in the curved space.

Disciplines

Physical Sciences and Mathematics | Physics

Comments

Suggested Citation:

C.D. Modes and R.D. Kamien. (2007). "Hard Disks on the Hyperbolic Plane." *Physical Review Letters*. **99**, 235701.

© 2007 The American Physical Society

<http://dx.doi.org/10.1103/PhysRevLett.99.235701>

Hard Disks on the Hyperbolic Plane

Carl D. Modes and Randall D. Kamien

Department of Physics and Astronomy, University of Pennsylvania, Philadelphia, Pennsylvania 19104-6396, USA
(Received 31 August 2007; revised manuscript received 2 October 2007; published 3 December 2007)

We examine a simple hard disk fluid with no long range interactions on the two-dimensional space of constant negative Gaussian curvature, the hyperbolic plane. This geometry provides a natural mechanism by which global crystalline order is frustrated, allowing us to construct a tractable model of disordered monodisperse hard disks. We extend free-area theory and the virial expansion to this regime, deriving the equation of state for the system, and compare its predictions with simulation near an isostatic packing in the curved space.

DOI: [10.1103/PhysRevLett.99.235701](https://doi.org/10.1103/PhysRevLett.99.235701)

The precise connections between the virial equation of state, the crystalline transition, glass transitions, and random close packing remain elusive [1,2]. The systematic calculation of the equation of state is perturbative and analytic in volume fraction, ϕ [3], and thus it is difficult to comprehend how it can, taken at face value, probe the nonanalytic, large volume fraction regime where crystallization occurs. At the other extreme, crystal free energies are well modeled by Kirkwood's free volume theory [4], especially near their maximum density. How can we probe, in three dimensions for instance, the crystalline phase transition in hard spheres at $\phi_X \approx 0.5$ and the possible existence of a maximally random jammed state near $\phi_{RCP} \approx 0.64$ [1,5]? Focusing on two-dimensional systems as a simple starting point is fraught with difficulties. Unlike the situation in three dimensions where local tetrahedral and icosahedral packing competes with global fcc crystallization [6], it is problematic to prevent crystallization in simulations of monodisperse disks [7], as triangular close packing is commensurate with crystalline order. Here we formulate the problem on a curved surface which serves to frustrate global crystalline order in a manner analogous to that in three dimensions. In particular, we study hard disks on the hyperbolic plane, \mathbb{H}^2 , at a curvature near a known regular tessellation. This model is numerically tractable and allows us to study the truly disordered regime, in contrast to the defect-laden, curved crystal where the defects themselves continue to exhibit an underlying order [6,8]. We find the equation of state for hard disks via molecular dynamics and compare our results to free-area theory for the packing derived from the nearby tessellation.

Experimentally, one could consider crystalline order and packing problems on any of the many bicontinuous structures in lipid and diblock phases [9] and present in the cell, such as the periodic cubic membrane in the mitochondria of *Chaos carolinensis* [10]. These bicontinuous structures, often close to minimal surfaces, have negative intrinsic curvature and the regular tessellations we consider here should serve as a scaffolding to model transitions on these surfaces.

On a two-dimensional manifold with constant intrinsic curvature K , the area of a circle of radius r is $a = A(r) =$

PACS numbers: 64.10.+h, 02.40.Ky, 05.20.Jj, 61.43.-j

$-2\pi K^{-1}[\cosh(\sqrt{-K}r) - 1] \rightarrow \pi r^2$ as $K \rightarrow 0$, as required. When we insert a disk of radius r onto our manifold, it excludes an area of radius $2r$ to the other disks. Thus the number of disks that cannot be inserted once the first disk is placed $A(2r)/A(r) \sim \exp\{\sqrt{-K}r\}$ grows exponentially with curvature and so we should expect that large, negative curvatures will lead to highly correlated disk packings due to the harsh entropic cost of this excluded area. Equivalently, the kissing number, n_{kiss} , the number of spheres which may simultaneously touch a central sphere grows with K [11]:

$$n_{\text{kiss}} = \frac{2\pi}{\cos^{-1}\left(\frac{\cosh(2\sqrt{-K}r)}{1 + \cosh(2\sqrt{-K}r)}\right)} \underset{K \rightarrow -\infty}{\sim} \pi e^{\sqrt{-K}r}. \quad (1)$$

To explore this systematically, we study the virial expansion for the pressure P in terms of the number density ρ , written $P = k_B T \sum_{n=1}^{\infty} B_n \rho^n$, where the B_1 term arises from the usual ideal gas law. While it may be tempting to assume $B_1 = 1$, the ideal gas on a curved manifold requires some thought; the circumference of a circle, $C(r) = 2\pi \sinh(\sqrt{-K}r)/\sqrt{-K}$, grows as fast as $A(r)$ making the infinite area, thermodynamic limit subtle.

The textbook approach to the ideal gas law begins with particle-in-a-box eigenenergies and takes the large area limit to calculate the partition function for a single particle, $Z_1 = V/\lambda_T^d$, where $\lambda_T = \sqrt{2\pi\hbar^2/(mT)}$ is the thermal wavelength. Fortunately, the spectrum of the Laplacian on a general Riemann surface has been well studied [12]. McKean and Singer [13] developed the Weyl expansion [14] for the partition function of a single particle on a periodic two-dimensional domain D :

$$Z_1(T) = \frac{1}{\lambda_T^2} \int_D dA \pm \frac{1}{4\lambda_T} \int_{\partial D} d\ell + \frac{1}{12\pi} \int_D K dA - \frac{1}{6\pi} \int_{\partial D} H d\ell + \mathcal{O}(\lambda_T), \quad (2)$$

where the sign of the first correction depends on Neumann (+) or Dirichlet (-) boundary conditions and H is the mean curvature. Now we see that the circumference directly affects B_1 and the only way to avoid the problem

with the boundary is to consider periodic boundary conditions, i.e., no boundary. We note that for hard disks the virial expansion includes only local interactions among clusters of particles. As long as the clusters in question do not wrap around the periodic space, we ignore the periodicity and perform the cluster integrals on \mathbb{H}^2 . In order to ensure that this is possible, we may continue to increase the area available to a cluster by constructing ever higher genus manifolds [15] and, thus, we can neglect “winding” of the disks around the periods. For manifolds with constant $K < 0$, $Z_1 = A[\lambda_T^{-2} + K/(12\pi)] > 0$ when $\lambda_T^2 < -12\pi/K$. In other words, we are forced to work in the regime where the curvature of the manifold does not probe the quantum regime of the gas. In this regime, the pressure $P = Nk_B T d \ln Z/dA$ is independent of the proportionality constant.

To calculate the virial coefficients, we employ the Poincaré disk model of \mathbb{H}^2 , popularized by Escher [16], which conformally maps the hyperbolic plane with curvature K to the disk of radius $\sqrt{-K^{-1}}$ on \mathbb{R}^2 . Using the complex coordinate $\zeta = x + iy$, the metric is $ds^2 = 4[1 + K\zeta\bar{\zeta}]^{-1}d\zeta d\bar{\zeta}$, where $\zeta\bar{\zeta} \leq -1/K$ [15]. Geodesics in this model are arcs of circles which intersect the bounding circle normally; circles in the hyperbolic plane remain circles in this model, but their coordinate centers and radii vary. The radius of curvature sets a length scale and, consequently, any system on \mathbb{H}^2 is manifestly not scale invariant.

We take advantage of this lack of scale invariance to probe higher curvatures not by changing the ambient space, but simply by considering larger and larger disks. We consider disks of radius $r\sqrt{-K}$. Without loss of generality we fix the Gaussian curvature to be $K = -1$. Dimensional analysis may always be employed to insert the appropriate factors of K . As in flat space, the second virial coefficient, $B_2(r)$, is given by half the excluded area of a single disk: $B_2(r) = \pi[\cosh(2r) - 1]$. As $r \rightarrow 0$ we recover the $d=2$ Euclidean result: $B_2(r) = (4\pi)^{(d/2)}r^d/[d\Gamma(\frac{d}{2})]$. Though it is tempting to associate the higher connectivity at larger curvatures with higher dimensions, we know of no natural identification.

We turn to numerical integration to evaluate the higher virial coefficients. In addition, as is traditional in flat space [17], the higher coefficients B_n are reported in units of $a^{n-1} = [A(r)]^{n-1}$ to suppress size effects and generate the expansion for $P/(\rho k_B T)$ in the area fraction, $\phi = \rho a$:

$$P = \rho k_B T \left[1 + \sum_{n=2}^{\infty} \frac{B_n}{a^{n-1}} \phi^{n-1} \right]. \quad (3)$$

We have checked the $r \rightarrow 0$ limit in all cases, and happily find agreement with the known Euclidean results. We plot B_2/a , B_3/a^2 , B_4/a^3 , and B_5/a^4 in Fig. 1 and see that the normalized virial coefficients grow rapidly with r , or equivalently, K . This demonstrates that the fluid phase quickly becomes correlated at ever higher curvatures. In

passing, we note that, to the accuracy of our calculation, B_3 and B_4 are positive, while B_5 may have a zero crossing. There is evidence that, in higher dimensional flat spaces, the virial coefficients alternate in sign [17,18] and hence the leading singularity that controls the radius of convergence of the expansion sits on the negative real axis [18]. The location of this singularity, and hence the range of applicability of the virial expansion itself, remains an open question in $D = 2, 3$. Whether or not $B_n(r)$ crosses zero for the negatively curved system at any value of r is the subject of future work.

Since our confidence in the reliability of the virial expansion wanes with ever larger curvature, both due to the numerics and the likelihood of growing higher-order corrections, we are forced to look at highly correlated structures on \mathbb{H}^2 . Free-area theory is the standard approach to ordered and disordered packings at high area fractions. With this in mind, we start by considering regular packings on the hyperbolic plane. We begin with a regular lattice of Voronoi cells and consider a tessellation of F p -gons, with q meeting at each vertex. The total number of vertices is pF/q , the total number of edges is $pF/2$, and the total number of faces is F . The Euler character χ of the surface constrains these three numbers and it follows that

$$\chi = V - E + F = pF \left[\frac{1}{q} + \frac{1}{p} - \frac{1}{2} \right]. \quad (4)$$

For the flat periodic plane (i.e., the torus) $\chi = 0$, and we find the three tilings represented by the Schläfli symbol $\{p, q\} = \{6, 3\}$, $\{3, 6\}$, and $\{4, 4\}$, hexagons, triangles, and squares, respectively. The spherical topology is the only one with positive $\chi = 2$, admitting the five Platonic solids $\{p, q\} = \{3, 3\}$, $\{3, 4\}$, $\{3, 5\}$, $\{4, 3\}$, and $\{5, 3\}$. Finally, we turn to the pertinent geometries with negative Gaussian curvature, for which $\chi < 0$ and $p^{-1} + q^{-1} < \frac{1}{2}$. In this case there are an infinite number of integral pairs $\{p, q\}$ and an infinite number of regular tessellations. Triangular packing around each vertex, $q = 3$, corresponds to close packing. We focus instead on isostatic packings, those for

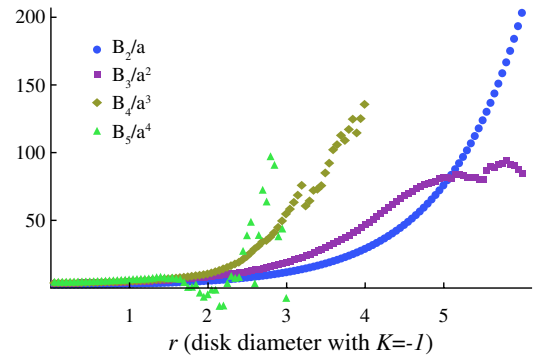


FIG. 1 (color online). The second, third, fourth, and fifth virial coefficients in appropriate units of the area, a , as functions of disk size (for $K = -1$) r .

which each disk has $p = 4$ nearest neighbors. Recall that an isostatic packing is one for which the number of force balance equations is equal to the number of degrees of freedom. For N frictionless particles in d dimensions with coordination z , there are dN degrees of freedom and $Nz/2$ forces to balance: isostaticity requires $z_c = 2d$ [19].

We find the area fraction of $\{p, q\}$ through application of the Gauss-Bonnet theorem and hyperbolic trigonometry. When there are F identical polygons, the area of each can be found from the Euler character χ : $FA_{p\text{-gon}} = \int dA = -\int KdA = -2\pi\chi$, where we have used $K = -1$. The radius of the in circle can be determined via the dual law of hyperbolic cosines [20], $\cosh(r) = \cos(\pi/q)/\sin(\pi/p)$. We find the area fraction for the $\{p, q\}$ tessellation:

$$\phi_{\{p,q\}} = \left[\frac{F}{\chi} \right] \left[1 - \frac{\cos(\pi/q)}{\sin(\pi/p)} \right]. \quad (5)$$

We recover the appropriate packing fractions, $\pi/3\sqrt{3}$, $\pi/4$, and $\pi/2\sqrt{3}$, for the Euclidean tilings, $\{3, 6\}$, $\{4, 4\}$, and $\{6, 3\}$, respectively. As $p \rightarrow \infty$ for close-packed $q = 3$ tessellations, we find $\phi_{\max} = 0.9549$, the known packing fraction of the best packing on the hyperbolic plane at any curvature [21]. The lowest packing fraction for an isostatic configuration ($p = 4$) is $\phi_{\text{iso}} = \phi_{\{4,\infty\}} = \sqrt{2} - 1 \approx 0.4142$, an area fraction far below that for the Euclidean square lattice $\pi/4 \approx 0.785$. Also of note is the broadening of the range in ϕ that supports stable configurations: $\phi_{\max} - \phi_{\text{iso}} \approx 0.54$ on \mathbb{H}^2 , as compared to a range of roughly 0.13 in flat space. This is consistent with our finding that the virial expansion breaks down at lower area fractions on \mathbb{H}^2 . Indeed, the $\{4, \infty\}$ tessellation requires $\cosh(r^*) = \sqrt{2}$ so that $B_2(r^*)/A(r^*) = \frac{1}{2}(2)/(\sqrt{2} - 1) = 1/\phi_{\{4,\infty\}}$. Though possibly a mathematical profundity, the fact that $B_2(r^*)\phi_{\{4,\infty\}}/A(r^*) = B_1$ means that the first correction to the ideal gas is precisely equal to the noninteracting result and strengthens the case that we must study the large ϕ regime.

The presence of these large corrections, even at low area fraction, necessitates an approach to the high-density regime. We turn to free-area theory, known to be exact near close packing [22,23]. In flat space, scale invariance ensures that the shape of the free-area region, available to each disk's center of mass, has precisely the same shape as the corresponding Voronoi cell. However, the rigidity of \mathbb{H}^2 forces us to consider how the shape of the cell changes as the size of the disks change. In Fig. 2 we show how we break up the Voronoi cell to calculate the resulting free area.

The free area can be found by starting with $A_{p\text{-gon}}$ and subtracting the area of each of the p strips, $A_{\text{strip}} = (s - 2\delta) \sinh(r)$ [24] and each of the p corners $A_{\text{corner}} = \pi - \alpha - 2\pi/q$. The hyperbolic law of cosines [20] allows us to find $\cosh \delta = \cos(\alpha/2) \csc(\pi/q)$, $\cosh s = [\cos(2\pi/p) + \cos^2(\pi/q)] \csc^2(\pi/q)$, and $\sin(\alpha/2) = \cos(\pi/q)/\cosh r$.

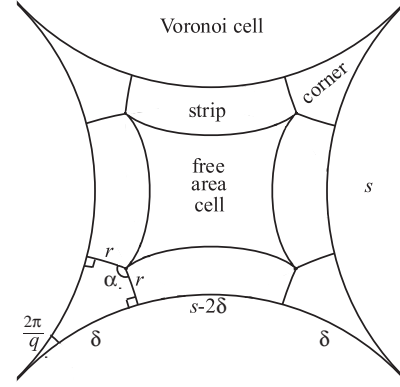


FIG. 2. Partition of a $\{p, q\}$ Voronoi cell into its free-area cell, p corners, and p strips. Note that the boundaries of the free-area cell are not geodesics.

We can relate r to ϕ , p , and q and write A_{free} in terms of p , q , and ϕ : setting $\tau = 1 - \frac{\chi\phi}{F}$ and $\tau_{pq} = 1 - \frac{\chi\phi_{\{p,q\}}}{F}$, we have

$$\begin{aligned} A_{\text{free}} = & 2p \sin^{-1} \left[\sin\left(\frac{\pi}{p}\right) \frac{\tau_{pq}}{\tau} \right] - 2\pi \\ & - 2p \sqrt{\tau^2 - 1} \cosh^{-1} \left[\frac{\cos(\frac{\pi}{p})}{\sin(\frac{\pi}{q})} \right] \\ & + 2p \sqrt{\tau^2 - 1} \cosh^{-1} \left[\frac{\sqrt{1 - \frac{\tau_{pq}^2}{\tau^2} \sin^2(\frac{\pi}{p})}}{\sin(\frac{\pi}{q})} \right]. \quad (6) \end{aligned}$$

Unfortunately, this expression is cumbersome to the point of uselessness, so we instead turn to Fig. 3, where we plot the free-area equations of state for various $\{p, q\}$ tessellations using $P_{\text{FA}} = -Ta^{-1}\phi^2 \frac{d}{d\phi} \ln(A_{\text{free}})$. Note that a is set by $A_{p\text{-gon}}\phi = a$.

Finally, we turn to disordered packings. We employed constant energy molecular dynamics on a periodic hyperbolic octagon with sides identified to give the topology of the 2-torus [15]. Note that we cannot vary ϕ by changing the disk size, as we must in free-area theory, since that is, by the absence of scale invariance, equivalent to a change in the background curvature. Instead, we change ϕ by changing the number of disks in the periodic octagon. We could choose a larger, higher genus periodic cell on which to do our simulation in which case we could probe a larger number of area fractions, filling in the data points in Fig. 3, though this is computationally intensive. Although the simulation and free-area theory share a common endpoint, the pressure in the latter samples ever-changing curvatures on its way to close packing. We choose to study curvatures $r = 0.53$ and $r = 0.531$, just below and just above that for the $\{4, 5\}$ tessellation, $r_{\{4,5\}} = 0.5306$. At these curvatures no regular tessellation is allowed, and so noncrystalline arrangements give the best packings [25]. Thus we expect to probe disordered configurations even at

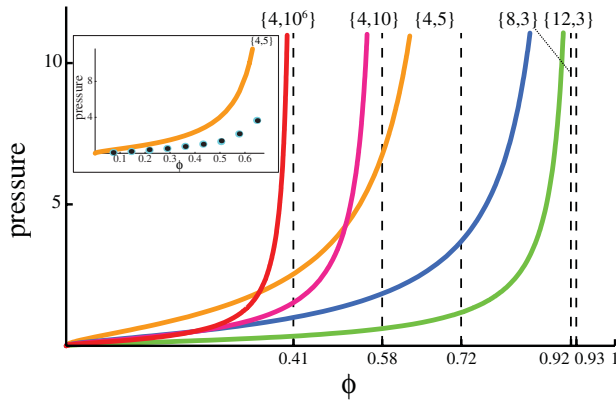


FIG. 3 (color online). The equation of state for free-area theory for a range of $\{p, q\}$ tessellations. Note that the pressure curves diverge at their maximum packing fractions and that they differ even at low area fractions, ϕ . The vertical dashed lines indicate the maximum area fraction for the tessellations listed on top of the figure. The inset compares our numerical results with the $\{4, 5\}$ free-area theory at larger values of the pressure. The larger (light blue) circles are the result of our molecular dynamics simulation for curvature just below the $\{4, 5\}$ tessellation and the smaller (black) circles are for curvature just above $\{4, 5\}$. The number of particles ranges from 1 to 9.

high densities with this choice. Indeed, the simulation suggests that the disordered system attains higher pressures less rapidly than the nearby, ordered, isostatic configurations, particularly at larger values of ϕ (Fig. 3). The $r \rightarrow 0$ limit should be a way to study these disordered packings on the Euclidean plane. Fortunately, roughly 10 disks fill the periodic octagon, the smallest periodic region on \mathbb{H}^2 , and thus we could quickly approach a dense packing. We require many more disks to study the Euclidean limit; this work is in progress.

We studied a hard disk gas through simulation, at curvatures close to that for a regular tessellation and compared with free-area theory. Thus we have a model which approaches disordered packings of monodisperse disks for which we can understand the equation of state. Note that our approach allows us to ponder the structure of the virial expansion: in d dimensions, the $2d^{\text{th}}$ virial coefficient, B_{2d} , is required to probe isostaticity, while crystallization requires the $n_{\text{kiss}}^{\text{th}}$ virial coefficient. Though increasing the dimension d pushes n_{kiss} ever larger [26], the study of disordered packings forces us to calculate ever more virial coefficients. The hyperbolic plane sidesteps this problem by keeping isostaticity at $p = 4$. Further work will focus on other tessellations, in particular, the Euclidean limit, and on mapping the results and predictions of \mathbb{H}^2 onto the bicontinuous structures present in biological systems.

It is a pleasure to acknowledge discussions with N. Clisby, C. Epstein, A. Liu, M. López de Haro,

B. McCoy, C. D. Santangelo, and D. Vernon. This work was supported in part by NSF Grant No. DMR05-47230, a gift from L. J. Bernstein, and a gift from H. H. Coburn. R. D. K. appreciates the hospitality of the Aspen Center for Physics where some of this work was done.

-
- [1] S. Torquato, T. M. Truskett, and P. G. Debenedetti, *Phys. Rev. Lett.* **84**, 2064 (2000).
 - [2] B. M. McCoy, arXiv:cond-mat/0103556v1.
 - [3] L. D. Landau and L. M. Lifshitz, *Statistical Physics* (Butterworth-Heinemann, Oxford, 1980), 3rd ed., pt. 1.
 - [4] J. G. Kirkwood, *J. Chem. Phys.* **18**, 380 (1950).
 - [5] R. D. Kamien and A. J. Liu, *Phys. Rev. Lett.* **99**, 155501 (2007).
 - [6] D. R. Nelson, *Phys. Rev. Lett.* **50**, 982 (1983).
 - [7] C. S. O'Hern *et al.*, *Phys. Rev. E* **68**, 011306 (2003).
 - [8] M. Kléman and J. F. Sadoc, *J. Phys. (Paris), Lett.* **40**, L569 (1979); See also J. F. Sadoc and R. Mosseri, *Geometrical Frustration* (Cambridge University Press, Cambridge, England, 1999).
 - [9] R. Hołyst, *Soft Matter* **1**, 329 (2005); *Nature Mater.* **4**, 510 (2005).
 - [10] Y. Deng and M. Mieczkowski, *Protoplasma* **203**, 16 (1998).
 - [11] M. Rubinstein and D. R. Nelson, *Phys. Rev. B* **28**, 6377 (1983).
 - [12] M. Kac, *Am. Math. Mon.* **73**, 1 (1966).
 - [13] H. P. McKean, Jr. and I. M. Singer, *J. Diff. Geom.* **1**, 43 (1967).
 - [14] H. Weyl, *Rend. Circ. Mat. Palermo* **39**, 1 (1915).
 - [15] F. Sausset and G. Tarjus, *J. Phys. A* **40**, 12 873 (2007).
 - [16] M. C. Escher, *Circle Limit III & Circle Limit IV*.
 - [17] M. Luban and A. Baram, *J. Chem. Phys.* **76** 3233 (1982).
 - [18] N. Clisby and B. M. McCoy, *Pramana J. Phys.* **64**, 775 (2005); *J. Stat. Phys.* **114**, 1343 (2004).
 - [19] J. C. Maxwell, *Philos. Mag.* **27**, 250 (1864); *Edinburg R. Soc. Trans.* **26**, 1 (1872).
 - [20] H. S. M. Coxeter, *Non-Euclidean Geometry* (The Mathematical Association of America, Washington, DC, 1998), 6th ed.
 - [21] H. S. M. Coxeter, *Twelve Geometric Essays* (Southern Illinois University Press, Carbondale, 1968).
 - [22] Z. W. Salsburg and W. W. Wood, *J. Chem. Phys.* **37**, 798 (1962).
 - [23] A. Donev, S. Torquato, and F. H. Stillinger, *Phys. Rev. E* **71**, 011105 (2005).
 - [24] T. H. Marshall and G. J. Martin, *Proc. Edinb. Math. Soc.* **46**, 67 (2003).
 - [25] L. Bowen and C. Radin, *Discrete Comput. Geom.* **29**, 23 (2002).
 - [26] A. D. Wyner, *Bell Syst. Tech. J.* **44**, 1061 (1965); see also J. H. Conway and N. J. A. Sloane, *Sphere Packings, Lattices and Groups* (Springer-Verlag, New York, 1988).